# Studying ZIF-8 SURMOF Thin Films with a Langatate Crystal Microbalance: Single-Component Gas Adsorption Isotherms Measured at Elevated Temperatures and Pressures

Elvia P. Valadez Sánchez, Alexander Knebel, Luis Izquierdo Sánchez, Michael Klumpp, Christof Wöll, and Roland Dittmeyer*

ABSTRACT: Characterizing the adsorption behavior of thin films at technical operation ranges is highly relevant in order to obtain appropriate experimental parameters, as well as to evaluate their possible integration in multiple applications. Nonetheless, gathering such experimental data is not a trivial task. In the case of metal−organic framework thin films, a particular interesting class of highly porous coatings, determination of adsorption isotherms at elevated temperatures and pressures is not commonly reported. Using a custom designed langatate crystal microbalance following the principle for piezoelectric microbalances, but under harsher conditions, allowed us to present adsorption equilibrium measurements on a zeolitic imidazolate framework 8 (ZIF 8) surface mounted metal−organic framework (SURMOF) thin film

at temperatures between 35 and 100 °C and at a pressure range up to 10 bars. The layer by layer liquid phase epitaxy approach was used to deposit ZIF 8 SURMOF thin films on langatate crystals. X ray diffraction, infrared reflection absorption spectroscopy, and scanning electron microscopy combined with energy dispersive X ray mapping were used to gather deeper information on the ZIF 8 thin film growth. Single component isotherms were collected for different gases of practical interest, that is, CO_2, C_2H_6, C_2H_4, C_3H_8, and C_3H_6. The measurements were obtained at 35, 50, 75, and 100 °C at a gauge pressure range up to 10 bars. The collected data showed a clear preferential adsorption of ethane over ethylene, whereas only a slight difference was found between propane and propylene. Additionally, the experimental data allowed for the determination of adsorption equilibrium constants and saturation loadings of the ZIF 8 material as a thin SURMOF film, which is of great importance for its integration in multiple applications, such as sensor devices or in membrane based separation.
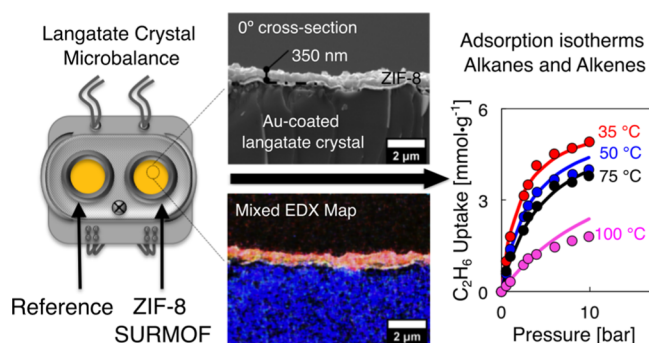
1. INTRODUCTION

Surface mounted metal−organic frameworks (SURMOFs) are porous materials typically of thin, highly oriented, and crystalline nature. They possess several advantages over conventional metal−organic framework (MOF) films includ ing controllable thicknesses, smoother morphologies, and lower defect densities.[1] Therefore, SURMOF thin films are particularly attractive and suitable for integration in diverse processes and devices, requiring high quality surfaces without the presence of pinholes or cracks,[2] for example, for sensing applications and membrane based separation.[3−5] When considering such applications, obtaining quantitative informa tion on their sorption behavior as well as the characteristics of the material within a technical operation range is crucial to truly assess its potential. Quartz crystal microbalances are commonly employed to study the adsorption behavior of microporous sorbents, such as MOFs, gravimetrically. None theless, quartz crystals have a known temperature limit close to 80 °C.[6] Langatate crystals resemble quartz but offer a broader temperature range of operation, permitting the study of a material's adsorption properties at higher temperatures.[7] A recent work succeeded in the study of the adsorption behavior of zeolite ZSM 5 using a crystal microbalance adapted for langatate crystals.[8] This proved the possibility of measuring and analyzing gas adsorption under harsher conditions.

Zeolitic imidazolate framework 8 (ZIF 8) is a highly known and explored MOF material belonging to the ZIF subclass. Its considerable thermal and mechanical stabilities, as well as its narrow sized windows of around 3.4 Å,[9] have made it a very interesting candidate for diverse applications, including gas

separation and heterogeneous catalysis.[10] For example, the exploration of alkane/alkene separation has been a focal point of study in various works, particularly given the similarity of the size of the windows with the kinetic diameters of short hydrocarbons.[11−13] To apply ZIF 8 in gas separation membranes, investigating its adsorption behavior at technical operation ranges is highly interesting. For instance, for ethylene/ethane and propylene/propane membrane splitters, typical operating temperatures and pressures vary from 30 to 100 °C and between 3 and 10 bar, respectively.[14] Looking at CO_2 capture from point sources via membranes, for example, for utilization as a chemical feedstock, for storage, or for sequestration, often operation temperatures of 100 °C or above are required at different pressures[15] in order to obtain attractive fluxes.

Nonetheless, in general, not much information about the adsorption behavior of MOF materials at high temperatures has been reported, particularly when speaking about thin films. As a matter of fact, to the best of our knowledge, the experimental determination of ZIF 8's gas adsorption behavior under both high temperatures and pressures has not yet been reported in the literature. In this work, we explore the high pressure and high temperature gas adsorption on a ZIF 8 SURMOF film for CO_2, C_2H_6, C_2H_4, C_3H_8, and C_3H_6 using a crystal microbalance adapted for langatate crystals (see Figure 1). The adsorption isotherms were obtained at 35, 50, 75, and
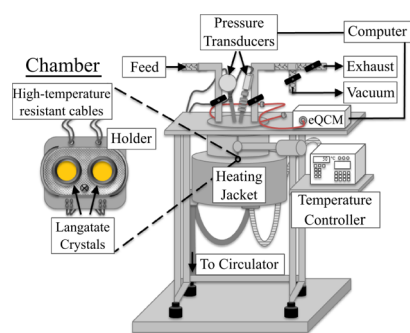

Figure 1. Schematic of the custom designed LCM for high temperature and high pressure adsorption measurements.

100 °C. The data collected were fitted to the Langmuir model in order to determine the adsorption equilibrium constants, saturation loadings, and heats of adsorption for the ZIF 8 material in a film at different temperatures. Such data are fundamental for a valid prediction of the performance of the ZIF 8 SURMOF thin films in multiple applications based on detailed simulation models.

2. EXPERIMENTAL SECTION

2.1. ZIF-8 SURMOF Synthesis. The ZIF 8 SURMOF was synthesized on a langatate crystal sensor (C3 Prozess und Analysentechnik GmbH, Munich, Germany) with a diameter of 14 mm, a finely lapped surface, Ti−Au electrodes, and a resonant frequency of 5 MHz. The crystal was initially cleaned in deionized water by ultrasonication for 5 min and then dried at 80 °C for 10 min. Afterward, the crystal was immersed in a 1 mM ethanolic solution of 11 mercapto 1 undecanol (Sigma Aldrich) for 24 h, in order to create a self assembled monolayer (SAM) with a hydroxide functionalized surface. Next, the crystal was rinsed with EtOH, dried with N_2, and placed in the appropriate holder to begin with the ZIF 8 SURMOF synthesis.

Following the layer by layer (LBL) liquid phase epitaxy approach, the thin film was deposited using a MSM Robust carousel tissue stainer device (Slee Thomas Medical, Austria); see Supporting Information Figure S1. Following the same synthesis routes as in previous studies,[16,17] the crystal was then sequentially immersed for 175 deposition cycles. Each cycle consisted of 4 dipping steps in methanolic solutions as follows: (1) 300 s in 10 mM zinc nitrate hexahydrate 98% (Alfa Aesar), (2) 100 s in MeOH (Merck SeccoSolv), (3) 300 s in 20 mM 2 methyl 1H imidazole (Merck), and (4) 100 s in MeOH (Merck SeccoSolv). After the completion of all the cycles, the sample was left inside the hood for drying.

The sample was then characterized with X ray diffraction (XRD) and infrared reflection absorption spectroscopy (IRRAS). For the XRD measurements, a D8 Advance diffractometer (Bruker) equipped with a Si strip detector (PSD Lynxeye) in $\theta−\theta$ geometry and variable divergence slit on the primary side applying Cu K$\alpha_{1,2}$ radiation with a wavelength of 0.15419 nm was employed. The measurements were recorded using a step width of $2\theta = 0.02°$ and 84 s per step over an angular range of $2\theta = 5.5−20°$. The IRRA spectra were recorded under ambient conditions using a Vertex 80 FTIR spectrometer (Bruker Optics) equipped with a liquid nitrogen cooled mercury cadmium telluride narrow band detector and a grazing incidence sample accessory providing an angle of 80° relative to the surface normal. The background measurements were performed using perdeuterated hexadecanethiol SAMs on gold coated silicon wafers.

Scanning electron microscopy (SEM) and energy dispersive X ray spectroscopy and mapping (EDXS, EDXM) were carried out using a TESCAN Vega 3 with a heated tungsten filament electron source and a Bruker XFlash 610M EDX detector. All images were made with 10 kV emission voltage with 8−10 μA emission current at a 14 mm working distance. For EDXM, the accumulation time was 30 min. To get the cross section, the sample was simply broken and glued to the cross section holder using conductive carbon glue tabs. Before the measurement, the sample was sputtered with a BalTec MCS 010 coating system with a sub nanometer coating of Au−Pd to reduce charging effects.

2.2. Langatate Crystal Microbalance. All adsorption measure ments were done using a custom designed langatate crystal holder inside of a 100 mL high pressure stainless steel chamber (Büchi AG, Uster, Switzerland) connected with high temperature resistant cables to a commercial frequency oscillating electrochemical quartz crystal microbalance 10 M (Gamry Instruments, Warminster, USA). This measurement system was already developed and validated in a previous work investigating the gas adsorption in zeolite H ZSM 5.[8,18] As it can be seen in Figure 1, the device holds two langatate crystals, one serving as the reference and the other as the sample. The pressure and temperature limits of the chamber are 300 bar and 275 °C, respectively; the latter is defined by the maximum operating temperature of the O rings (Kalrez 6375) which ensure a sealed chamber at high pressures. The pressure in the system is regulated by two different pressure transducers of 0−1 bar absolute (Haenni) and 0−60 bar gauge (WIKA, Klingenberg, Germany). The temperature in the system is set with a btc 01 temperature controller (Büchi AG, Uster, Switzerland) connected to thermocouples close to the crystals. During the experiments conducted, the temperature regulator reached precisions of ±0.1 °C at 35 °C, ±0.25 °C at 50 °C, ±0.35 °C at 75 °C, and ±0.4 °C at 100 °C.

2.3. Reference Measurements. The device holds two crystals. One is the neat crystal and serves as a reference, while the other one is the ZIF 8 coated crystal, that is, the sample. Before beginning with adsorption measurements and prior to any synthesis, both—uncoated—crystals were placed in the holder, the chamber was then closed gas tight, evacuated, and purged with N_2 three times. The crystals were then activated overnight under vacuum at 75 °C. Following, the resonant frequencies of the two—uncoated—crystals were recorded for 35, 50, 75, and 100 °C over a gauge pressure range between 0 and 10 bar. These pressures were adjusted by introducing N_2 via a mass flow controller into the chamber. This step is of great importance because there are always variations between different langatate crystals, which cause a frequency difference, Δf_r. This

difference must be defined prior to film deposition for all parameter sets—in terms of temperature and pressure—to be investigated. This will permit, later on, the accurate determination of the adsorbed mass. In addition, these reference measurements are also important for being able to account for the dependency of the resonant frequency on temperature and pressure.[8] The frequency difference is then given as

$$\Delta f_r = f_{1,r} - f_{2,r} \qquad (1)$$

where $f_{1,r}$ is the resonant frequency of the first "uncoated" crystal, and $f_{2,r}$ is the resonant frequency of the second "uncoated" crystal before adsorption measurements.

2.4. Gas Uptake Measurements. After the reference measurements, one of the crystals was removed from the holder and treated as specified above in the ZIF 8 2.1 section. After the synthesis of the ZIF 8 SURMOF was confirmed (see Figure 2), the "coated" crystal or sample was placed once again in the holder. Likewise, the chamber was then closed gas tight, evacuated, and purged with N_2 three times. The reference crystal and the sample were then activated under vacuum at the first temperature to be measured, that is, 35 °C. Next and before introducing the gas to be studied, an initial measurement, in order to determine the mass of the film on the "coated" crystal, was performed. Afterward, the gas to be measured was dosed to achieve

a)

b)

c) Tilt angle= 40°
100 μm

d) Tilt angle= 15°
10 μm

e) 0° Cross-section
350 nm
ZIF-8
Au-coated Langatate-Crystal
2 μm

f)
2 μm

g) O-K Au-Mαβ Ga-L La-Lα
C-K N-Kα Zn-L

Figure 2. (a) XRD pattern and (b) IRRAS spectra of the ZIF 8 SURMOF sample studied in this work synthesized on a langatate crystal for 175 deposition cycles; cross sectional SEM images of a second ZIF 8 SURMOF sample deposited for 175 cycles on the langatate crystal (c) with 40° tilt angle and (d) with 15° tilt angle; (e) high resolution 0° tilt angle cross section with the 350 nm ZIF 8 layer; (f) corresponding mixed EDX map; and (g) EDX maps of the elements.

each desired pressure point. Once the desired pressure was reached and the temperature was stabilized, the resonant frequencies for the reference and the sample were measured. This was done over a gauge pressure range of 0−10 bar for CO_2, C_2H_6, and C_2H_4 and of 0−1.35 bar for C_3H_8 and C_3H_6. This exact procedure was then repeated for 50, 75, and 100 °C. Following, the change in frequency, Δf, was determined by

$$\Delta f = f_1^* - f_2 = f_1 - \Delta f_r - f_2 \qquad (2)$$

where f_1^* is the resonant frequency of the reference, f_1 is the resonant frequency of the reference during adsorption measurements, and f_2 is the resonant frequency of the sample during adsorption measurements.

The shift in frequency is the summation of various independent terms such as temperature, pressure, and viscosity as well as "roughness loading".[8,19] However, given that both samples were measured together in the same chamber and therefore under the same conditions, such frequency changes were considered negligible. Thus, a shift in frequency in the hereby presented work is solely attributed to changes in mass, that is, $\Delta f = \Delta f_m$. Considering this and using the Sauerbrey equation,[20] the deposited mass of the ZIF 8 SURMOF on the langatate crystal was first determined.

$$\Delta m = \frac{n \cdot \Delta f_m \cdot \sqrt{\rho_1 \cdot \mu_1}}{2(f_1^*)^2} \cdot A \qquad (3)$$

where Δm is the difference in mass in grams, $n = 3$ is the number of the harmonic driving the langatate crystal, $\rho_1 = 6.13$ g·cm^{-3} corresponds to the density of the langatate crystal, $\mu_1 = 1.9 \times 10^{12}$ g·cm^{-1}·s^{-2} is the effective piezoelectrically stiffened shear modulus of the langatate crystal, and $A = 1.54$ cm^2 corresponds to the area of the langatate crystal.[7,21] As explained above, this was the first step before the dosing of every gas. In the present work, the deposited mass of the ZIF 8 SURMOF on the langatate crystal was determined to be 0.049 mg considering the average value of all the measurements at 35−75 °C. Likewise, the same formula was then used to determine the gas adsorption for each measurement point.

3. RESULTS AND DISCUSSION

As the results from XRD and IRRAS analysis show (cf. Figure 2a,b), ZIF 8 as the SURMOF was successfully grown on the langatate crystal using the LBL deposition method. In the IRRAS spectrum, the characteristic bands of ZIF 8 in Figure 2b could be identified. From the XRD in Figure 2a, good crystallinity of the ZIF 8 SURMOF on the surface could be also observed, considering the fact that the surface roughness of the underlying langatate crystal is high, as distinguishable in the cross sectional overview SEM images of a second sample (cf. Figure 2c,d). The sample is coated very homogenously; however, it was very challenging to find a part of the sample where the high resolution cross sectional image (Figure 2e) showed an almost flat surface. The corresponding EDXM in Figure 2f and the single element maps in Figure 2g give a good idea of the overall structure of the substrate: the langatate crystal shows the elements Ga, La, and O in the EDX as expected; Ta was left out of the mixed map because of its low concentration in the sample. In the top layer, attributed to ZIF 8, C and N from the linker (2 methylimidazole) are found. Zn, which is the metal source for the MOF, is found in the whole sample, that is, the langatate crystal contains Zn too. Still, given that in the Au layer no Zn is found, the presence of Zn on the top MOF layer can be affirmed. Furthermore, because of the sputtering process, the Au signal is found throughout the sample, nevertheless with the highest concentration right below the MOF layer because of the gold coating of the langatate crystal. Overall, the EDXM analysis provided a good
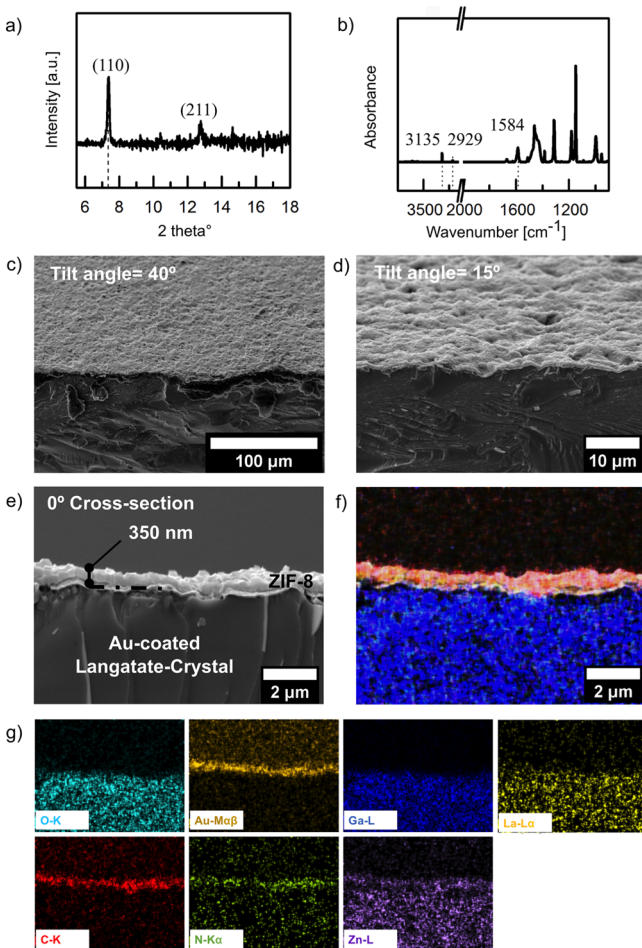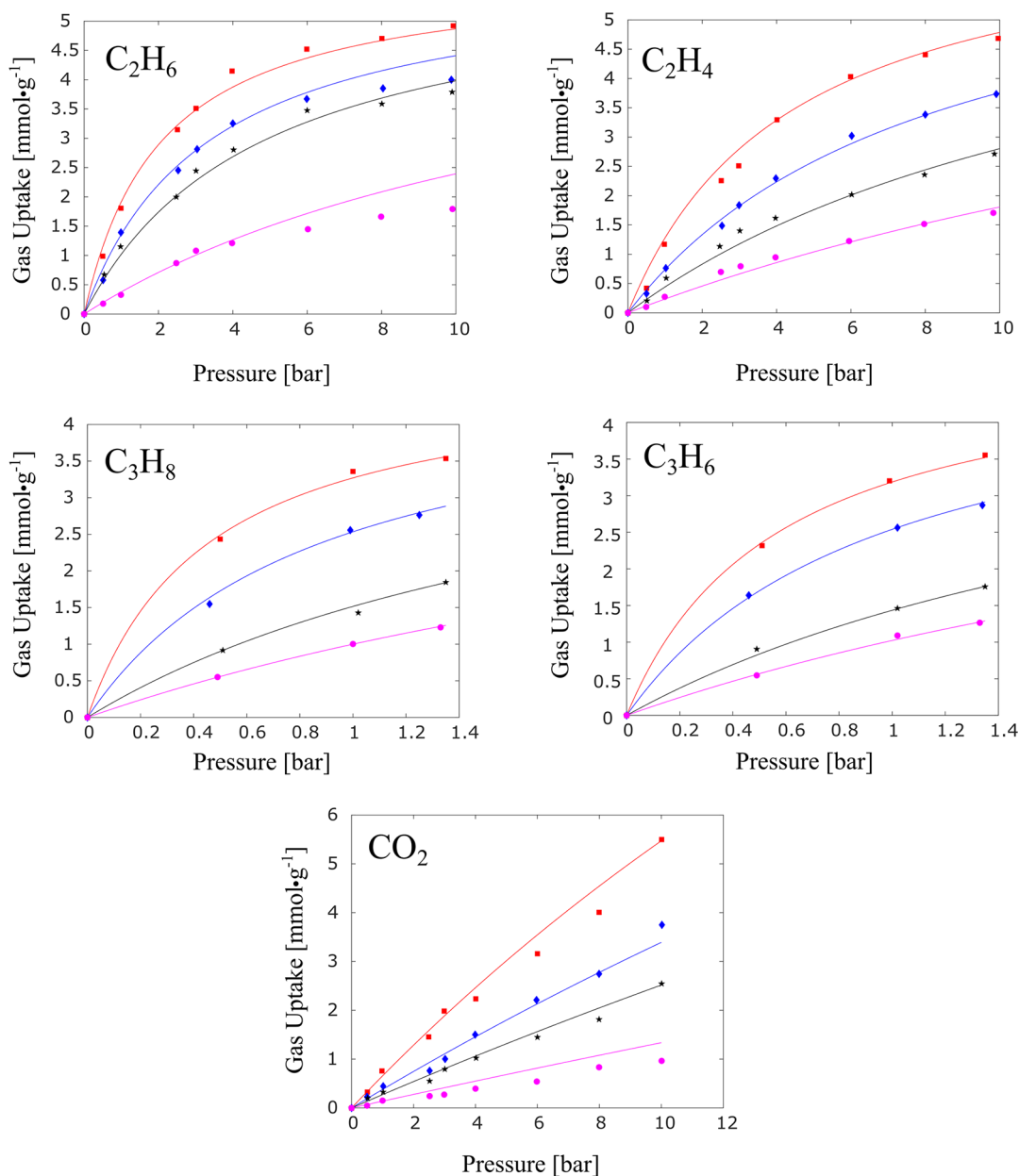
Figure 3. Mean loadings for C_2H_6, C_2H_4, C_3H_8, and C_3H_6 in the ZIF 8 SURMOF at 35 °C (red ■), 50 °C (blue ◆), 75 °C (black ★), and 100 °C (pink ●) fitted (solid line) to the Langmuir model.

qualitative insight on the ZIF 8 layer, deposited on top of the langatate crystal.

Next, in order to verify the accuracy of the langatate crystal microbalance (LCM) and therefore the reliability of the data deduced, adsorption experiments at 35 °C were conducted for CO_2, C_2H_6, C_2H_4, C_3H_8, and C_3H_6. The data obtained is in good agreement with the other published adsorption isotherms for ZIF 8.[22−26] Considering alkanes and alkenes, these studies (experiments conducted at 20−35 °C) report the following ranges at 1 bar: 1−2.5 mmol/g^{-1} for C_2H_6, 0.7−1.6 mmol/g^{-1} for C_2H_4, 3.6−4.4 mmol/g^{-1} for C_3H_8, and 2.7−4.5 mmol/g^{-1} for C_3H_6. Moreover, molecular simulations and experimental studies have reported that the strongest adsorption sites in ZIF 8 are in the surroundings of the linkers.[27−29]

To continue with the analysis of the adsorption data, mean loadings were determined for all gases from the two replicate measurements; these correspond to the markers shown in

Figure 3. While the adsorption equilibrium constants, K_T; T = 35, 50, 75, and 100 °C, are temperature dependent, the saturation loadings, q_{sat}, are theoretically temperature inde pendent for the simple monolayer Langmuir isotherm.[30] For this reason, the five corresponding Langmuir parameters of each gas, that is, $K_{35°C}$, $K_{50°C}$, $K_{75°C}$, $K_{100°C}$, and q_{sat}, were estimated at the same time with the total data collected, rather than independently for each temperature. Furthermore, the parameters were estimated by minimizing the weighted sum of squares, with the weights being the inverse of the squared standard deviation of each of the corresponding measure ments; in case of no deviation within the measurements, the standard deviation was assumed to be 5% of the mean loading. For the estimation, the lsqnonlin function of MATLAB was used. Additionally, 95% likelihood confidence intervals were also determined (see Supporting Information Figure S2, Tables S1−S10). The obtained Langmuir fittings are shown

in solid lines in Figure 3. When compared to the reported literature, C_2 hydrocarbon isotherms have been commonly identified to present a Henry type behavior.[26,31] Nonetheless, for the pressure and temperature range explored in this work, all single component adsorption isotherms could be generally described with the simple Langmuir model. The corresponding adsorption equilibrium constants and saturation loadings are reported in Table 1. In general, the obtained saturation

Table 1. Saturation Loadings, q_{sat}, and Adsorption Equilibrium Constants, K_T, for C_2H_6, C_2H_4, C_3H_8, C_3H_6, and CO_2 in the ZIF 8 SURMOF at Different Temperatures

Langmuir parameters		C_2H_6	C_2H_4	C_3H_8	C_3H_6	CO_2
q_{sat}	[mmol g^{-1}]	5.87	6.88	4.76	5.01	29.47
$K_{35°C}$	[bar^{-1}]	0.48	0.23	2.19	1.75	0.02
$K_{50°C}$	[bar^{-1}]	0.30	0.12	1.14	1.03	0.01
$K_{75°C}$	[bar^{-1}]	0.21	0.07	0.47	0.4	0.009
$K_{100°C}$	[bar^{-1}]	0.07	0.04	0.27	0.26	0.005

loadings for the C_2 and C_3 hydrocarbons are slightly below from what is reported in the literature.[22,32,33] On the other hand, the saturation loading for CO_2 appears to be higher than expected, considering other experimental and simulated studies that have reported CO_2 adsorption isotherms (25−35 °C) in ZIF 8 at even higher pressures (25−30 bar).[22,34] Future studies should focus on improving further the precision of these estimates, for example, with a larger amount of data, lower standard deviations, and a larger pressure range.

Continuing with the discussion of the data, the amount of adsorbed gas decreased in all the cases with increasing temperatures. Considering only the last mean loading points for each gas and taking 35 °C as the starting experiment, a decrease in the amount of gas adsorbed of around 22, 43, and 68% was observed for the 50, 75, and 100 °C isotherms, respectively.

When comparing the behavior of alkanes and alkenes, it can be observed that the ZIF 8 SURMOF exhibited a preferential alkane adsorption for the C_2 hydrocarbons. Considering the difference in the amount adsorbed, the equilibrium selectivity ($\alpha = K_{C_2H_6}/K_{C_2H_4}$) was estimated to be the highest (approx. 3.1) at 75 °C and lowest (approx. 1.9) at 100 °C. In general, the preferential adsorption of alkanes over alkenes in ZIF 8 has been reported earlier in several studies and identified as a common finding for cation free nonpolar structures;[12,23,26] such behavior can be attributed to molecular polarizability.[26] The experiments in this work support once again this observation for thin ZIF 8 films at higher temperatures and pressure regions. In contrast, simulation studies conducted for higher pressures (above 10 bar)[12,32] have shown that further increasing the pressure results in a higher alkene uptake. Wu et al.[32] explained that such behavior might be related to the smaller size of the alkene, that is, as the pressure continues to rise, the smaller molecule is more capable of accessing the ZIF 8 pores, thus reaching higher uptakes. In the hereby presented work, pressures above 10 bar were not explored; thus, such behavior could not be confirmed.

For the C_3 hydrocarbons, that is, for C_3H_8 and C_3H_6, only a gauge pressure range of up to 1.35 bar was explored. The limitations behind these measurements come from the setup itself, which did not permit to achieve higher pressures for these gases. The adsorption isotherms obtained presented

generally the same uptake, that is, very slight differences in adsorption could be observed as the pressure was increased, which agrees with multiple literature data.[23,25,33] Furthermore, compared to C_2 hydrocarbons, not only the relative uptake of C_3 hydrocarbons in ZIF 8 was significantly higher in the low pressure region investigated for both species, but also the gradient was larger. Herm et al.[35] discussed some common trends in MOFs, including that smaller sized alkanes possess lower adsorption strength given their lower molecular surface area for van der Waal interactions. Moreover, in the work by Zhang et al.[33] adsorption isotherms for n C_4H_{10} and 1 C_4H_8 were also reported. The isotherms exhibited extremely similar behaviors and higher uptakes when compared to C_3H_8 and C_3H_6 at low pressures. Thus, as suggested earlier by Böhme et al.,[23] the interaction strength in ZIF 8 does appear to increase with the hydrocarbon chain length, at least at a low pressure range (below 1 bar). Likewise, Zhang et al.[36] identified a stronger affinity of the ZIF 8 framework to longer chain hydrocarbons. On the other hand, the preferential adsorption of the alkane over the alkene appears to be reduced with increasing chain length.

Next, the heats of adsorption for the alkanes and alkenes in the ZIF 8 SURMOF were estimated via the van't Hoff equation

$$K = K_0 \, e^{-\Delta H_s/RT} \tag{4}$$

where K_0 is a pre exponential factor, and H_s is the heat of adsorption;[26] for van't Hoff plots ($\ln K$ vs $1/T$) please refer to the Supporting Information Figures S3 and S4. Considering only the Henry type region for the C_2 hydrocarbon isotherms, where the guest−host interactions govern sorption,[37] heats of adsorption of 18.1 and 19.5 kJ·mol^{-1} for C_2H_4 and C_2H_6 were respectively estimated. These values are in line with the literature data ranging between 15 and 20 kJ·mol^{-1}.[26,31] When considering the whole pressure range explored in this work, that is, using K_L, higher values (26.5 kJ·mol^{-1} for C_2H_4 and 26.9 kJ·mol^{-1} for C_2H_6) were obtained. For the C_3 hydrocarbons, the heats of adsorption were estimated using the Langmuir constants given the data available. In the case of C_3H_6 and C_3H_8, the heats of adsorption obtained were of 29.1 and 31.2 kJ·mol^{-1}, respectively which are in excellent agreement with multiple studies ranging between 25 and 34 kJ·mol^{-1}.[37−40] With all of the data collected in this work, better theoretical models for real world applications might be obtained: models that take molecular sieving,[41] adsorption heat/energies, and molecular lattice vibrations into account.[42]

To finalize, all of the results presented in this work correspond to the characterization of a ZIF 8 SURMOF film, information highly relevant when considering its integration in thin film and coating technologies. Further measurements at temperatures above 100 °C were no longer conducted for the ZIF 8 SURMOF film studied in this work, as it could be observed that the mass deposited in the sensor started to decrease (ca. 5%) during the 100 °C experiments. Likewise, its crystallinity and composition were also compromised. This provided an insight into the behavior of the material when exposed to noninert gases under harsh operation conditions. Long term experiments at the different pressure and temperature conditions explored in this work are of high interest to obtain further information on the film's degradation limits.

4. CONCLUSIONS

The adsorption of diverse gases at elevated temperatures and pressures on a ZIF 8 SURMOF film was investigated in this work via a crystal microbalance adapted for langatate sensors. Experimental findings for the ZIF 8 SURMOF film showed a preferential adsorption of the alkane over the alkene for the C_2 hydrocarbons, while similar adsorption uptakes for the C_3 hydrocarbons. The adsorption uptake in ZIF 8 increased with the hydrocarbon chain length, while the adsorption affinity for the alkane over the alkene was reduced as the chain length increased. In general, all of the single component adsorption isotherms could be described with the Langmuir model; future studies should focus on further improving the accuracy of the measurements, for example, by covering an even larger pressure range. The heats of adsorption obtained from these data when considering the low pressure region were of 18.1 and 19.5 kJ·mol^{-1} for C_2H_4 and C_2H_6 and of 29.1 and 31.2 kJ·mol^{-1} for C_3H_6 and C_3H_8, respectively. Significant variations in the adsorption uptake could also be noticed with increasing temperatures, which can be of particular interest for systems involving C_2H_6 and C_2H_4, considering the known preferential diffusion of C_2H_4 competing against the preferential adsorption of C_2H_6. Furthermore, a decrease in mass deposited could be observed during the measurements at 100 °C, for which further experiments were not conducted.

Even though the collection of the experimental data over a wide range of conditions may not always be a trivial task, determining diverse parameters, such as saturation loadings and adsorption equilibrium constants, is fundamental for the creation and improvement of theoretical models. In the case of uptake measurements, the device used in this work proved as an attractive option for the deeper characterization of SURMOF films and other materials under harsh environments closer to those of real world applications. Additionally, the use of this device to study the long term stability of materials and the effect on its adsorption properties is highly interesting, particularly for new SURMOF structures with a demonstrated potential.

AUTHOR INFORMATION

Corresponding Author

Roland Dittmeyer − *Institute for Micro Process Engineering (IMVT) and Institute of Catalysis Research and Technology (IKFT), Karlsruhe Institute of Technology (KIT), 76344 Eggenstein Leopoldshafen, Germany;*

Email: roland.dittmeyer@kit.edu; Fax: +49 721 608 23186

Authors

Elvia P. Valadez Sánchez − *Institute of Functional Interfaces (IFG) and Institute for Micro Process Engineering (IMVT), Karlsruhe Institute of Technology (KIT), 76344 Eggenstein Leopoldshafen, Germany*

Alexander Knebel − *Institute of Functional Interfaces (IFG), Karlsruhe Institute of Technology (KIT), 76344 Eggenstein Leopoldshafen, Germany;*

Luis Izquierdo Sánchez − *Institute for Micro Process Engineering (IMVT), Karlsruhe Institute of Technology (KIT), 76344 Eggenstein Leopoldshafen, Germany*

Michael Klumpp − *Institute for Micro Process Engineering (IMVT) and Institute of Catalysis Research and Technology (IKFT), Karlsruhe Institute of Technology (KIT), 76344 Eggenstein Leopoldshafen, Germany;*

Christof Wöll − *Institute of Functional Interfaces (IFG), Karlsruhe Institute of Technology (KIT), 76344 Eggenstein Leopoldshafen, Germany;*

ABBREVIATIONS

SURMOFs, surface mounted metal−organic framework; MOF, metal−organic framework; ZIF 8, zeolitic imidazolate framework 8; MUD, 11 mercapto 1 undecanol; SAM, self assembled monolayer; LBL, layer by layer; LPE, liquid phase epitaxy; XRD, X ray diffraction; IRRAS, infrared reflection absorption spectroscopy; MCT, mercury cadmium telluride; SEM, scanning electron microscopy; EDXS, EDXM, energy dispersive X ray spectroscopy and mapping; eQCM, electro chemical quartz crystal microbalance; LCM, langatate crystal microbalance

REFERENCES

(1) Heinke, L.; Tu, M.; Wannapaiboon, S.; Fischer, R. A.; Wöll, C. Surface mounted metal organic frameworks for applications in sensing and separation. *Microporous Mesoporous Mater.* **2015**, *216*, 200−215.

(2) Zhuang, J. L.; Terfort, A.; Wöll, C. Formation of oriented and patterned films of metal−organic frameworks by liquid phase epitaxy: A review. *Coord. Chem. Rev.* **2016**, *307*, 391−424.

(3) Bétard, A.; Fischer, R. A. Metal−organic framework thin films: from fundamentals to applications. *Chem. Rev.* **2011**, *112*, 1055−1083.

(4) Zacher, D.; Schmid, R.; Wöll, C.; Fischer, R. A. Surface chemistry of metal−organic frameworks at the liquid−solid interface. *Angew. Chem., Int. Ed.* **2011**, *50*, 176−199.

(5) Allendorf, M. D.; Houk, R. J. T.; Andruszkiewicz, L.; Talin, A. A.; Pikarsky, J.; Choudhury, A.; Gall, K. A.; Hesketh, P. J. Stress Induced Chemical Detection Using Flexible Metal−Organic Frameworks. *J. Am. Chem. Soc.* **2008**, *130*, 14404−14405.

(6) Tsionsky, V.; Gileadi, E. Use of the quartz crystal microbalance for the study of adsorption from the gas phase. *Langmuir* **1994**, *10*, 2830−2835.

(7) Davulis, P. M.; Da Cunha, M. P. High temperature langatate elastic constants and experimental validation up to 900 °C. *IEEE Trans. Ultrason. Ferroelectr. Freq. Control* **2010**, *57*, 59−65.

(8) Ding, W.; Klumpp, M.; Li, H.; Schygulla, U.; Pfeifer, P.; Schwieger, W.; Haas Santo, K.; Dittmeyer, R. Investigation of high temperature and high pressure gas adsorption in zeolite H ZSM 5 via the langatate crystal microbalance: CO_2, H_2O, methanol, and dimethyl ether. *J. Phys. Chem. C* **2015**, *119*, 23478−23485.

(9) Park, K. S.; Ni, Z.; Côté, A. P.; Choi, J. Y.; Huang, R.; Uribe Romo, F. J.; Chae, H. K.; O'Keeffe, M.; Yaghi, O. M. Exceptional chemical and thermal stability of zeolitic imidazolate frameworks. *Proc. Natl. Acad. Sci. U.S.A.* **2006**, *103*, 10186−10191.

(10) Lee, Y. R.; Jang, M. S.; Cho, H. Y.; Kwon, H. J.; Kim, S.; Ahn, W. S. ZIF 8: A comparison of synthesis methods. *Chem. Eng. J.* **2015**, *271*, 276−280.

(11) Rungta, M.; Zhang, C.; Koros, W. J.; Xu, L. Membrane based ethylene/ethane separation: The upper bound and beyond. *AIChE J.* **2013**, *59*, 3475−3489.

(12) Bux, H.; Chmelik, C.; Krishna, R.; Caro, J. Ethene/ethane separation by the MOF membrane ZIF 8: molecular correlation of permeation, adsorption, diffusion. *J. Membr. Sci.* **2011**, *369*, 284−289.

(13) Valadez Sánchez, E. P.; Gliemann, H.; Haas Santo, K.; Ding, W.; Hansjosten, E.; Wohlgemuth, J.; Wöll, C.; Dittmeyer, R. α Al_2O_3 supported ZIF 8 SURMOF membranes: Diffusion mechanism of ethene/ethane mixtures and gas separation performance. *J. Membr. Sci.* **2020**, *594*, 117421.

(14) Benali, M.; Aydin, B. Ethane/ethylene and propane/propylene separation in hybrid membrane distillation systems: Optimization and economic analysis. *Sep. Purif. Technol.* **2010**, *73*, 377−390.

(15) Míguez, J.; Porteiro, J.; Pérez Orozco, R.; Gómez, M. Technology Evolution in Membrane Based CCS. *Energies* **2018**, *11*, 3153.

(16) Valadez Sánchez, E. P.; Gliemann, H.; Haas Santo, K.; Wöll, C.; Dittmeyer, R. ZIF 8 SURMOF Membranes Synthesized by Au Assisted Liquid Phase Epitaxy for Application in Gas Separation. *Chem. Ing. Tech.* **2016**, *88*, 1798−1805.

(17) Valadez Sánchez, E. P. *Thin Film MOFs (SURMOFs) for Application in Gas Separation*; KIT Scientific Publishing, 2019.

(18) Ding, W.; Baracchini, G.; Klumpp, M.; Schwieger, W.; Dittmeyer, R. Adsorption Device Based on a Langatate Crystal Microbalance for High Temperature High Pressure Gas Adsorption in Zeolite H ZSM 5. *J. Visualized Exp.* **2016**, No. e54413.

(19) Tsionsky, V.; Daikhin, L.; Urbakh, M.; Gileadi, E. Behavior of quartz crystal microbalance in nonadsorbed gases at high pressures. *Langmuir* **1995**, *11*, 674−678.

(20) Sauerbrey, G. Verwendung von Schwingquarzen zur Wägung dünner Schichten und zur Mikrowägung. *Z. Phys.* **1959**, *155*, 206−222.

(21) Ding, W. *Simulation Assisted Design of Polycrystalline Zeolite Catalysts*; KIT Scientific Publishing, 2016.

(22) Shekhah, O.; Swaidan, R.; Belmabkhout, Y.; Du Plessis, M.; Jacobs, T.; Barbour, L. J.; Pinnau, I.; Eddaoudi, M. The liquid phase epitaxy approach for the successful construction of ultra thin and defect free ZIF 8 membranes: pure and mixed gas transport study. *Chem. Commun.* **2014**, *50*, 2089−2092.

(23) Böhme, U.; Barth, B.; Paula, C.; Kuhnt, A.; Schwieger, W.; Mundstock, A.; Caro, J.; Hartmann, M. Ethene/ethane and propene/propane separation via the olefin and paraffin selective metal organic framework adsorbents CPO 27 and ZIF 8. *Langmuir* **2013**, *29*, 8592−8600.

(24) Su, W.; Zhang, A.; Sun, Y.; Ran, M.; Wang, X. Adsorption Properties of C2H4 and C3H6 on 11 Adsorbents. *J. Chem. Eng. Data* **2016**, *62*, 417−421.

(25) Pimentel, B. R.; Lively, R. P. Enabling kinetic light hydrocarbon separation via crystal size engineering of ZIF 8. *Ind. Eng. Chem. Res.* **2016**, *55*, 12467−12476.

(26) James, J. B.; Wang, J.; Meng, L.; Lin, Y. S. ZIF 8 membrane ethylene/ethane transport characteristics in single and binary gas mixtures. *Ind. Eng. Chem. Res.* **2017**, *56*, 7567−7575.

(27) Chmelik, C.; Freude, D.; Bux, H.; Haase, J. Ethene/ethane mixture diffusion in the MOF sieve ZIF 8 studied by MAS PFG NMR diffusometry. *Microporous Mesoporous Mater.* **2012**, *147*, 135−141.

(28) Wu, H.; Zhou, W.; Yildirim, T. Methane Sorption in Nanoporous Metal−Organic Frameworks and First Order Phase Transition of Confined Methane. *J. Phys. Chem. C* **2009**, *113*, 3029−3035.

(29) Zhou, M.; Wang, Q.; Zhang, L.; Liu, Y. C.; Kang, Y. Adsorption sites of hydrogen in zeolitic imidazolate frameworks. *J. Phys. Chem. B* **2009**, *113*, 11049−11053.

(30) Ruthven, D. M. *Principles of Adsorption and Adsorption Processes*; John Wiley & Sons, 1984.

(31) Krokidas, P.; Castier, M.; Economou, I. G. Computational study of ZIF 8 and ZIF 67 performance for separation of gas mixtures. *J. Phys. Chem. C* **2017**, *121*, 17999−18011.

(32) Wu, Y.; Chen, H.; Liu, D.; Qian, Y.; Xi, H. Adsorption and separation of ethane/ethylene on ZIFs with various topologies: Combining GCMC simulation with the ideal adsorbed solution theory (IAST). *Chem. Eng. Sci.* **2015**, *124*, 144−153.

(33) Zhang, C.; Lively, R. P.; Zhang, K.; Johnson, J. R.; Karvan, O.; Koros, W. J. Unexpected molecular sieving properties of zeolitic imidazolate framework 8. *J. Phys. Chem. Lett.* **2012**, *3*, 2130−2134.

(34) Liu, D.; Wu, Y.; Xia, Q.; Li, Z.; Xi, H. Experimental and molecular simulation studies of CO_2 adsorption on zeolitic imidazolate frameworks: ZIF 8 and amine modified ZIF 8. *Adsorption* **2013**, *19*, 25−37.

(35) Herm, Z. R.; Bloch, E. D.; Long, J. R. Hydrocarbon Separations in Metal−Organic Frameworks. *Chem. Mater.* **2014**, *26*, 323−338.

(36) Zhang, L.; Li, Q.; Lu, Z.; Wang, X. Understanding Adsorption and Separation behavior of shorter chain alkane mixtures in Zeolitic Imidazolate Frameworks by molecular simulations. *Procedia Comput. Sci.* **2011**, *4*, 1193−1202.

(37) Krokidas, P.; Castier, M.; Moncho, S.; Brothers, E.; Economou, I. G. Molecular simulation studies of the diffusion of methane, ethane, propane, and propylene in ZIF 8. *J. Phys. Chem. C* **2015**, *119*, 27028−27037.

(38) Liu, D.; Ma, X.; Xi, H.; Lin, Y. S. Gas transport properties and propylene/propane separation characteristics of ZIF 8 membranes. *J. Membr. Sci.* **2014**, *451*, 85−93.

(39) Hara, N.; Yoshimune, M.; Negishi, H.; Haraya, K.; Hara, S.; Yamaguchi, T. Diffusive separation of propylene/propane with ZIF 8 membranes. *J. Membr. Sci.* **2014**, *450*, 215−223.

(40) Li, K.; Olson, D. H.; Seidel, J.; Emge, T. J.; Gong, H.; Zeng, H.; Li, J. Zeolitic imidazolate frameworks for kinetic separation of propane and propene. *J. Am. Chem. Soc.* **2009**, *131*, 10368−10369.

(41) Zheng, B.; Pan, Y.; Lai, Z.; Huang, K. W. Molecular dynamics simulations on gate opening in ZIF 8: identification of factors for ethane and propane separation. *Langmuir* **2013**, *29*, 8865−8872.

(42) Knebel, A.; Geppert, B.; Volgmann, K.; Kolokolov, D. I.; Stepanov, A. G.; Twiefel, J.; Heitjans, P.; Volkmer, D.; Caro, J. Defibrillation of soft porous metal organic frameworks with electric fields. *Science* **2017**, *358*, 347−351.